



1  
2  
3  
4  
5  
6  
7  
8  
9  
10  
11  
12  
13  
14  
15  
16  
17  
18  
19  
20  
21  
22  
23  
24  
25  
26  
27  
28  
29  
30  
31

## North Atlantic sea level budget revisited

**Zhe Song<sup>1,2</sup>, Anny Cazenave<sup>1</sup>, William Llovel<sup>2</sup>, Andrea Storto<sup>3</sup> and Marie Bouih<sup>4</sup>**

<sup>1</sup>Université de Toulouse, LEGOS (CNES/CNRS/IRD/UT3), 31401 Toulouse, CEDEX 9, France

<sup>2</sup>Université de Bretagne Occidentale, CNRS, Ifremer, IRD, Laboratoire d'Océanographie Physique et Spatiale (LOPS), IUEM, 29280, Plouzané, France

<sup>3</sup>Institute of Marine Science, National Research Council of Italy, Rome, Italy

<sup>4</sup>Magellium, 31520 Ramonville St Agne, France

*Correspondence to:* Zhe Song ([zhe.song@univ-brest.fr](mailto:zhe.song@univ-brest.fr)) and Anny Cazenave ([anny.cazenave@univ-tlse3.fr](mailto:anny.cazenave@univ-tlse3.fr), [anny.cazenave@gmail.com](mailto:anny.cazenave@gmail.com))

Submitted to Ocean Science

February 2026



## 32 **Abstract**

33 Based on satellite altimetry, GRACE space gravimetry and Argo-based steric data down to  
34 2000m, recent studies have shown that the North Atlantic sea level budget (i.e., altimetry-based  
35 sea level minus sum of components) of the past two decades is not closed, with strong regional  
36 residuals in the North Atlantic. This was suggested to result from salinity errors reported since  
37 ~2015 in some Argo float measurements. In this study, we revisit the North Atlantic sea level  
38 budget, using satellite altimetry, GRACE and GRACE-FO data, different Argo products and  
39 two ocean reanalyses (CIGAR and ORAS5) over the 2004-2022 time span. The ocean  
40 reanalyses are used to estimate the manometric contribution, an alternative to using GRACE  
41 data, as well as the deep ocean contribution to the sea level budget, not yet fully sampled by  
42 Argo. Analyzing different data sets allows us to evaluate their impact on the previously  
43 reported non-closure of the North Atlantic sea level budget. We first find that using the CIGAR  
44 ocean reanalysis-based manometric component significantly reduces the residuals of the North  
45 Atlantic sea level budget compared to GRACE. We also find that accounting for the deep ocean  
46 (below 2000m) thermal expansion (using the CIGAR reanalysis) allows for 30% reduction of  
47 the North Atlantic budget residuals when using GRACE for the manometric component, while  
48 the mean residual trend is reduced by a factor of 2 when using CIGAR for the manometric sea  
49 level. In the latter case, the budget is closed within data uncertainties. The North Atlantic  
50 halosteric component based on Argo and CIGAR in the upper 2000m displays a small decrease  
51 since the early 2010s. However, this negative trend becomes stronger after 2016. The 2010–  
52 2016 halosteric decrease may reflect a real salinity increase in the region, although salinity  
53 measurement errors may have impacted the halosteric component after that date.

54



## 55 **1 Introduction**

56 While many studies have been devoted to assessing the global mean sea level budget over the  
57 satellite altimetry era (1993 to present) (e.g., Barnoud et al., 2021; Bouih et al., 2025; Chen et  
58 al., 2020; Dieng et al., 2017; Horwath et al., 2022; Llovel et al., 2023; Nerem et al., 2018;  
59 WCRP, 2018) , only a few have focused on the regional sea level budget, with mixed results  
60 (e.g., Bouih et al., 2025; Camargo et al., 2023; Frederikse et al., 2016; Hamlington et al., 2020;  
61 Mu et al., 2024; Royston et al., 2020). At the global scale, the main terms of the sea level budget  
62 are the global mean sea level rise and ocean mass (known as barystatic sea level, Gregory et  
63 al., 2019) and thermosteric chang. At regional scale, however, other factors play a non-  
64 negligible role, such as the halosteric (i.e., salinity-related) component, which makes the  
65 regional sea level budget more complex to assess. In effect, a spurious salinity drift (giving rise  
66 to an important halosteric component decrease) has been reported recently in some Argo-based  
67 measurements (Liu et al., 2020; Ponte et al., 2021; Wong et al., 2023), that is supposed to have  
68 a strong impact on the closure assessment of the regional sea level budget. Considering all  
69 ocean basins, a recent study (Bouih et al., 2025) investigated the regional sea level trend budget  
70 closure over the 2004-2022 time span, using altimetry-based sea level data, GRACE space  
71 gravimetry for the regional ocean mass variations (also called manometric component, Gregory  
72 et al., 2019) and Argo data for the steric (sum of thermosteric and halosteric terms) component  
73 down to 2000m (global mean trends removed from all data sets). Bouih et al. (2025) also  
74 considered several ocean reanalyses to compute the manometric component (an alternative to  
75 using GRACE data), following the approach developed by Camargo et al. (2023), i.e., using  
76 the sterodynamic sea level (Gregory et al., 2019) computed by the reanalysis and correcting it  
77 for the local steric effect. The Bouih et al. (2025)'s study showed that in the Pacific, Indian and  
78 South Atlantic Oceans, the sea level budget trend residuals (altimetry-based sea level minus  
79 sum of components) were non-significant, considering the data uncertainties. On the other hand,  
80 strong positive residuals were found in the North Atlantic, whatever the manometric



81 component considered (i.e., either from GRACE or from the ocean reanalyses). These authors  
82 suspected the Argo-based spurious halosteric component (impacted by the Argo-based salinity  
83 drift) as the cause of the non-closure of the sea level budget in the North Atlantic.

84 In the present study we revisit the question of the North Atlantic sea level budget over the  
85 2004-2022 time span, using a variety of different data sets for the components of the sea level  
86 budget: different GRACE mascon solutions and different Argo-based gridded products down  
87 to 2000m, as well as two ocean reanalyses that provide an estimate of the steric signal from the  
88 deep ocean. Our objective is to evaluate the impact of each product on the currently reported  
89 non-closure of the North Atlantic sea level budget. An important addition compared to the  
90 Bouih et al. (2025)'s study, indeed consists of accounting for the deep ocean warming below  
91 2000m (not sampled by Argo) using estimates from the ocean reanalyses. This paper is  
92 organized as follows. Section 2 presents the data and analysis method. Section 3 displays the  
93 results for the North Atlantic sea level budget, both in terms of trend maps and time series. The  
94 sea level budget excluding the North Atlantic (average over all other oceans) is also briefly  
95 discussed in that section. A synthesis of the results is presented in the Discussion section  
96 (section 0) with some highlights on the few main messages arising from this study.

## 97 **2 Data and methods**

### 98 **2.1 Data**

#### 99 *2.1.1 Altimetry-based total sea level*

100 Sea level variations have been continuously measured by satellite altimetry since 1993. In this  
101 study, we use the daily  $0.25^\circ \times 0.25^\circ$  gridded sea level anomaly data, version DT2021 available  
102 from the Copernicus Climate Change Service (C3S) (<https://cds.climate.copernicus.eu/>). The  
103 data set is further corrected for the TOPEX-A instrumental drift that affected the first 6 years  
104 of the time series, but the correction has no impact on our assessment that starts in 2004. The



105 Jason-3 radiometer drift that impacts the wet troposphere correction (Brown et al., 2023) is  
106 corrected for. The altimetry data set is also corrected for the absolute Glacial Isostatic  
107 adjustment (GIA) effect, using the ICE6G-D model from Peltier et al. (2018).

### 108 *2.1.2 GRACE-based ocean mass*

109 The Gravity Recovery and Climate Experiment (GRACE) and GRACE Follow-On (GRACE-  
110 FO) are joint missions by the National Aeronautics and Space Administration (NASA) and the  
111 German Aerospace Center (DLR) (Tapley et al., 2019). These satellites have been measuring  
112 temporal variations in Earth's gravity field since 2002. This data set is essential for estimating  
113 mass redistribution in the oceans, terrestrial water storage, ice sheets, and glaciers.  
114 GRACE/GRACE-FO data are generally available in two forms: Spherical Harmonic (SH)  
115 coefficients and Mass Concentration (mascon) solutions. In this study, we utilize the latest  
116 Release 6 (RL06) mascon solutions provided by three different institutions: the Center for  
117 Space Research (CSR), the Jet Propulsion Laboratory (JPL), and the German Research Centre  
118 for Geosciences (GFZ). These mascon solutions, at monthly temporal resolution, are corrected  
119 for the geocentric motion (degree-1) using the Sun et al. (2016) solution. The  $C_{20}$  and  $C_{30}$   
120 coefficients are derived from Satellite Laser Ranging (SLR) data. The GIA correction for  
121 GRACE is based on the ICE6G-D model from (Peltier et al. (2018). Additionally, the GAD  
122 product derived from AOD1B models (Dobslaw et al., 2017; Flechtner et al., 2014), which  
123 represents non-tidal atmospheric and oceanic mass redistribution, is added back over the ocean  
124 areas to restore the ocean bottom pressure, which combines the effects of ocean mass and  
125 atmospheric loading. For alignment with altimetry-based sea level data which are corrected for  
126 the inverse barometer, we remove the global mean atmospheric pressure at every grid mesh in  
127 GRACE/GRACE-FO ocean mass data using the spatial mean of the GAD product at each  
128 month (Chen et al., 2019). In this study, we both use individual mascon solutions as well as  
129 their ensemble mean.



### 130 *2.1.3 Argo-based gridded data*

131 The Argo program is an international observational network that deploys a global array of  
132 autonomous profiling floats to measure temperature and salinity in the upper 2000m of the  
133 ocean. Several institutions process the raw data from these floats and publish gridded  
134 temperature (T) and salinity (S) data. In this study, we utilize three distinct gridded products:  
135 the Scripps Institution of Oceanography (SIO, Roemmich and Gilson, 2009), the Japan Agency  
136 for Marine-Earth Science and Technology (JAMSTEC, Hosoda, 2007), and the Met Office  
137 Hadley Centre (EN4 product, version 2.2, Cheng et al., 2014). Note that the SIO product rejects  
138 salinity profiles exceeding a difference of 0.1 psu when comparing to historical estimate based  
139 on the WOCE Global Hydrographic Climatology (Roemmich and Gilson, 2009). This  
140 correction tends to withdraw the salinity drift reported in Argo floats since 2016 (Liu et al.,  
141 2020; Ponte et al., 2021; Wong et al., 2023). Note that the other two products do not apply such  
142 a correction. All three data products are available at <https://argo.ucsd.edu/data/data-access/>  
143 (downloaded in October 2025). The thermosteric, halosteric and total steric sea level time series  
144 are computed from these gridded temperature and salinity data using the Gibbs SeaWater  
145 (GSW) Oceanographic Toolbox (McDougall et al., 2011) which implements the 2010  
146 Thermodynamic Equation Of Seawater (TEOS-10) standard. The gridded Argo-based time  
147 series have a spatial resolution of  $1^{\circ} \times 1^{\circ}$  at monthly interval over January 2004 to December  
148 2022.

### 149 *2.1.4 Ocean reanalyses*

150 We also used two ocean reanalysis data sets: (1) the CNR-ISMAR Global Historical Reanalysis  
151 (CIGAR, Storto and Yang, 2024), and (2) the Ocean Reanalysis System 5 (ORAS5, Zuo et al.,  
152 2019) available from the Copernicus Climate Change Service  
153 (<https://www.copernicus.eu/en/copernicus-services>).



154 CIGAR is a reanalysis system developed by Storto and Yang (2024). It is based on the NEMO  
155 ocean model version 4.0.7 (<https://www.nemo-ocean.eu/>) and is forced by the ECMWF ERA5  
156 atmospheric reanalysis (<https://www.ecmwf.int/en/forecasts/dataset/ecmwf-reanalysis-v5>).  
157 The system uses a three-dimensional variational (3D-Var) scheme to assimilate in situ profiles  
158 from the EN4 data set. Notably, CIGAR does not assimilate satellite altimetry data, which  
159 allows for independent comparisons. The system consists of 32 ensemble members generated  
160 through varying configurations (e.g., perturbed initial conditions and atmospheric forcing). In  
161 this study, we use the ensemble mean of the 32 members to derive the thermosteric, halosteric  
162 and steric sea level.  
163 The ORAS5 ocean reanalysis is based on the NEMO model (v3.4.1) and uses the NEMOVAR  
164 data assimilation system. It assimilates a wide range of observations, including satellite  
165 altimetry and sea surface temperature, at an eddy-permitting resolution of  $0.25^\circ \times 0.25^\circ$ .

## 166 **2.2 Methods**

### 167 *2.2.1 Computation of the manometric component*

168 In this study, we utilize two methods to obtain an estimate of the manometric component. One  
169 method is to use the ensemble mean of the GRACE mascon solutions from CSR, JPL, and  
170 GSFC to obtain the GRACE-based manometric estimate. The other method, an alternative to  
171 using GRACE solutions, relies on ocean reanalysis data and follows the approach developed  
172 by Camargo et al. (2023). Here, we use the sterodynamic sea level provided by the CIGAR  
173 ocean reanalysis, which combines the global mean thermosteric and dynamic sea level changes.  
174 To isolate the manometric component, we subtract the local steric effect from the sterodynamic  
175 sea level and further add the contemporary Gravitational, Rotational, and Deformation (GRD)  
176 fingerprints (representing solid Earth deformations and gravitational effects due to present-day  
177 land ice melt and terrestrial water storage changes; Gregory et al., 2019), to obtain a  
178 manometric component comparable to GRACE. The sea level fingerprint data used in this



179 study are based on monthly GRD fingerprint grids ( $0.5 \times 0.5$  resolution) estimated by Adhikari  
180 et al. (2019). Since this original dataset ends in 2016, we extended the time series up to 2022  
181 using linear extrapolation, assuming that the observed trend remains constant after 2016 (see  
182 Bouih et al., 2025 for details). This reanalysis-based estimate is hereafter referred to as CIGAR  
183 manometric. Manometric sea level change generally refers to the sea level component  
184 associated with ocean mass variations (i.e., excluding the steric component). It is driven by  
185 water mass exchange with the continents (such as land ice melt and terrestrial water storage  
186 changes) as well as mass redistribution within the ocean, driven by ocean circulation. However,  
187 in the context of this study, we focus exclusively on the internal mass redistribution component  
188 (with the global mean ocean mass trend removed). Therefore, the 'manometric sea level' here  
189 refers solely to the redistribution by the ocean circulation, of water mass already present in the  
190 oceans, with the GRDs effect added as explained above.

191

### 192 *2.2.2 Post processing of the data*

193 To ensure spatial consistency across all observing systems, all gridded data sets were spatially  
194 interpolated onto a  $1^\circ \times 1^\circ$  grid and averaged at monthly interval. A three-month moving  
195 average filter was applied to the time series. For the spatial analysis, a common mask was  
196 applied to all gridded components to exclude regions with high uncertainty. This mask covers  
197 latitudes from  $66^\circ\text{S}$  to  $66^\circ\text{N}$ , excludes inland seas, and omits coastal regions where the distance  
198 from land is less than 300 km (see Bouih et al., 2025 for details). Seasonal signals (annual and  
199 semi-annual) are removed from the time series through a least-squares adjustment of 6 and 12-  
200 month sinusoids. For the spatial maps, this least-squares fit was used to calculate the trends at  
201 each grid point. Finally, the globally averaged trend of each data set computed over the study  
202 period was subtracted from each grid point before constructing the spatial trend maps to focus  
203 on regional spatial patterns. The study period spans from January 2004 to December 2022.



### 204 2.2.3 Data uncertainties

205 For the altimetry grids, we use the uncertainties estimated by Prandi et al. (2021). For the  
206 GRACE-based manometric component, uncertainties are derived from the dispersion of the  
207 data sets with respect to the ensemble mean. For the CIGAR-based manometric, thermosteric,  
208 halosteric and steric data, the dispersion of the 32 realizations around the ensemble mean was  
209 used to estimate the uncertainties. For the residual time series, the uncertainty was estimated  
210 using the law of error propagation, considering all terms of the sea level budget. Regarding the  
211 trend uncertainty, it is expressed as the standard error of the least-squares fit. To obtain the  
212 uncertainty at the 95% confidence level, we scaled the standard error by a factor of 2  
213 (representing the 2-sigma interval).

## 214 3 Results

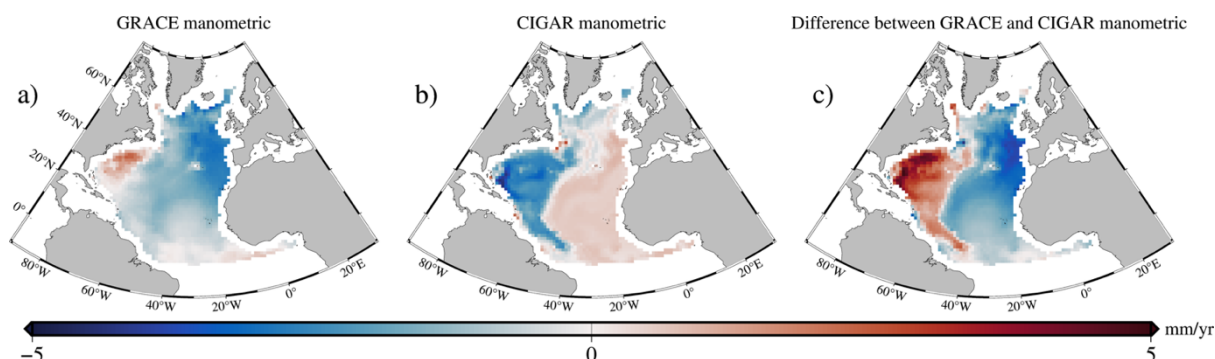
### 215 3.1 Comparison of the different manometric components over the North Atlantic

216 Figure 1a, b, shows the spatial manometric trend in the North Atlantic using the GRACE and  
217 CIGAR manometric data. Comparing Figure 1(a) and (b), we observe distinctly contrasting  
218 patterns between the GRACE and CIGAR manometric components. For the GRACE-based  
219 component, significant negative trends dominate most of the basin, with magnitudes gradually  
220 weakening from east to west. However, positive trends are observed in the western tropical  
221 Atlantic. In contrast, the CIGAR manometric component displays positive trends in the east  
222 and negative trends in the west, separated by a distinct dividing line, which likely corresponds  
223 to the position of the Mid Atlantic Ridge. This contrast is clearly illustrated Figure 1c, which  
224 plots the difference between the GRACE and CIGAR estimates. The results indicate that the  
225 GRACE manometric trends are larger than those of CIGAR west of 40°W, particularly along  
226 the eastern coast of North America. Conversely, in the region east of 40°W, the GRACE



227 manometric trends are smaller than the CIGAR trends, with the most significant difference  
228 observed near Greenland.

229



230

231 *Figure 1. Manometric sea level trends in the North Atlantic over 2004.01-2022.12 derived from*  
232 *(a) the mean of three GRACE mascon solutions and (b) the CIGAR ocean reanalysis. (c)*  
233 *Difference between (a) and (b).*

234

### 235 **3.2 Comparison of the different steric products over the North Atlantic**

236 Figure 3a-c shows the thermosteric sea level (TSL) trends over 2004-2022 over the North  
237 Atlantic for the three Argo products SIO, JAMSTEC and EN4. Similarly, Figure 3d-f shows  
238 the halosteric sea level (HSL) trends for the same data sets and period. As expected, due to  
239 thermohaline compensation particularly strong in the North Atlantic (e.g., Pardaens et al., 2011;  
240 Wang et al., 2010; Wunsch et al., 2007), the two components display opposite trends.  
241 Regarding the thermosteric component (Figure 3a-c), while all three products display similar  
242 spatial patterns, their magnitudes vary. The JAMSTEC and EN4 products show stronger  
243 positive trends around 20°N compared to the SIO product. However, all three products indicate  
244 significant positive signals in the eastern North Atlantic. The three halosteric products share  
245 similar spatial patterns; however, the magnitude of the SIO product is notably smaller than for  
246 JAMSTEC and EN4, the latter two being very similar. This difference likely results from the

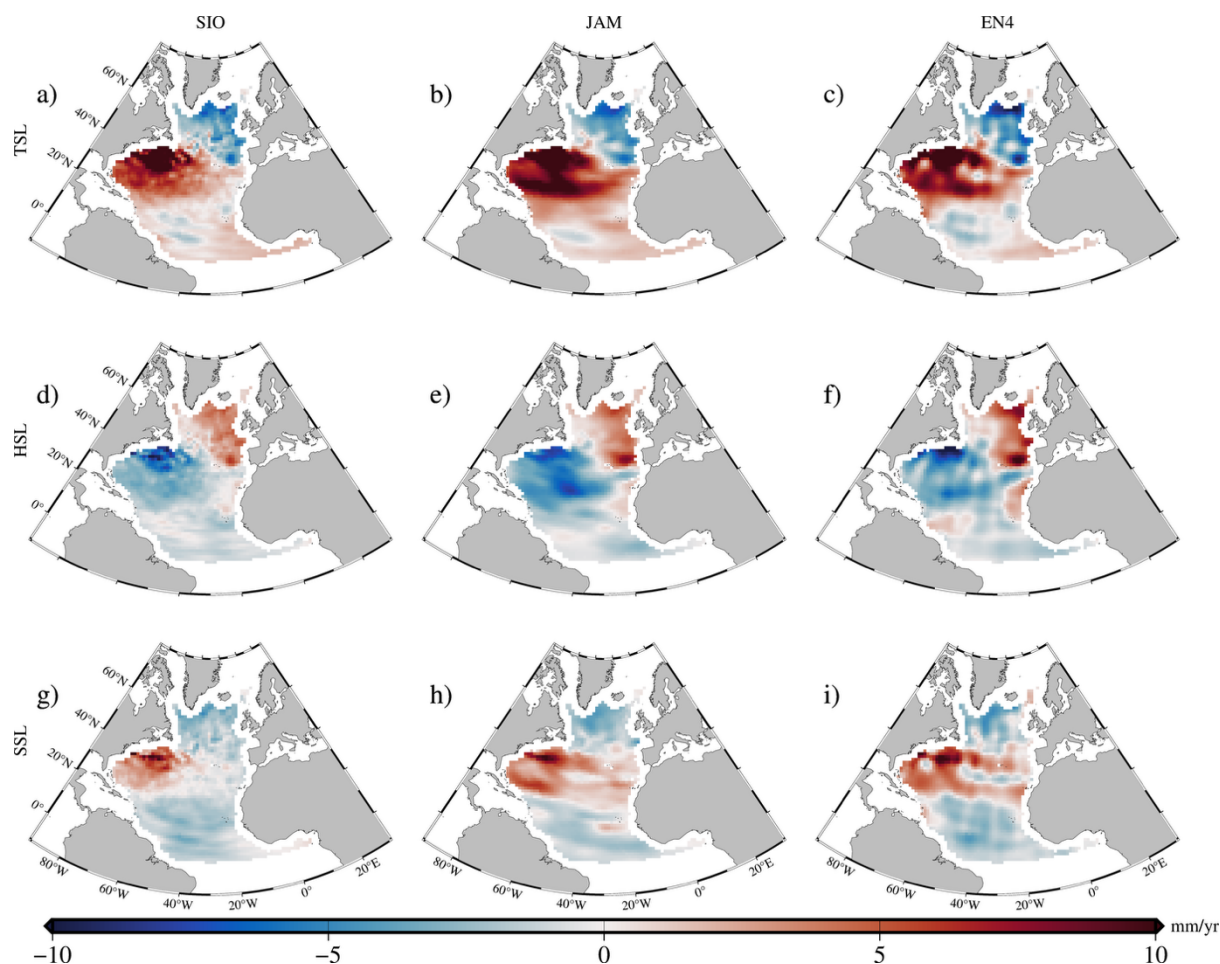


247 SIO processing that corrects for the instrumental salinity drift reported in Argo floats since  
248 2016, whereas the other products may not account for this. The mapping methods used by the  
249 different processing groups, in particular the assumed different correlation radii, may also  
250 contribute to the observed differences.

251 The steric sea level (SSL) trends are shown in Figure 3g-i. The magnitude of the total steric  
252 change is smaller than that of the thermosteric component alone. This implies that the halosteric  
253 contribution plays a significant compensatory role in the North Atlantic (consistent with  
254 previous published studies (e.g., Bouih et al., 2025; Llovel and Hochet, 2025). Unlike in the  
255 case of the global mean, the influence of salinity changes on sea level cannot be ignored in this  
256 region.

257

258



259

260 *Figure 2. Trends of thermosteric (a–c), halosteric (d–f), and steric (g–i) sea level change in*  
261 *the North Atlantic over 2004–2022 derived from the SIO (a, d, g), JAMSTEC (b, e, h), and EN4*  
262 *(c, f, i) Argo products.*

263

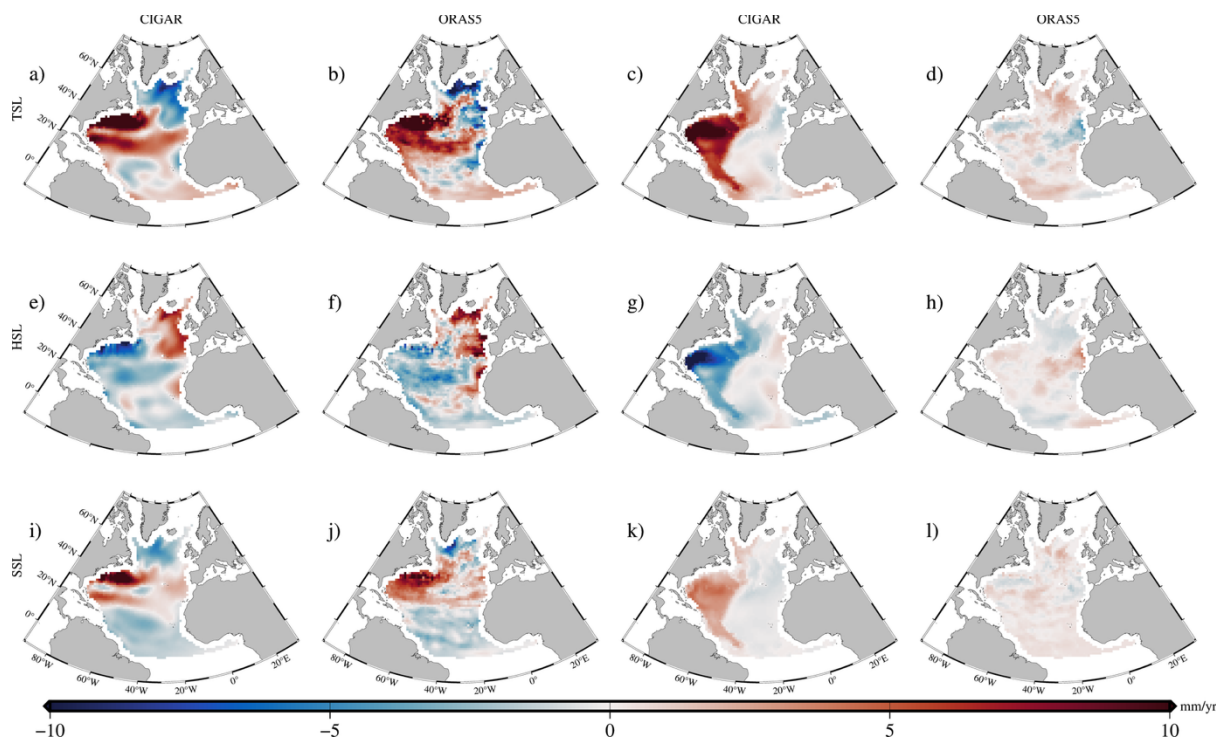
### 264 3.2.1 Ocean reanalyses-based thermosteric, halosteric and steric products

265 In addition to Argo products, we used the CIGAR and ORAS5 ocean reanalysis data to compute  
266 thermosteric, halosteric, and steric sea level changes for both the upper 2000m and the deep



267 ocean (2000m-6000m), as shown in Figure 3. In the upper 2000m, CIGAR and ORAS5 exhibit  
268 similar spatial patterns across all three components. Notably, the thermosteric sea level change  
269 displays a significant signal in the western North Atlantic, consistent with the Argo-based  
270 results. However, marked discrepancies between the two reanalyses are evident below 2000m.  
271 The CIGAR product displays strong positive thermosteric and negative halosteric signals in  
272 the western North Atlantic compared to ORAS5. In contrast, the deep ocean signals in ORAS5  
273 are weak and spatially incoherent, with some areas showing even signs opposite to those  
274 observed in the upper 2000m. Consequently, the spatial patterns in CIGAR, triggered by  
275 vertical physics and, to a lesser extent, vertical error correlations embedded in the 3D-Var  
276 scheme, appear more consistent with the upper 2000m than those in ORAS5.

277



278

279 *Figure 3. Trends of thermosteric (a–d), halosteric (e–h), and steric (i–l) sea level change in*  
280 *the North Atlantic over 2004–2022. The panels compare contributions from the upper 2000 m*



281 *(a, b, e, f, i, j) and below 2000 m (c, d, g, h, k, l) derived from the CIGAR (a, c, e, g, i, k) and*  
282 *ORAS5 (b, d, f, h, j, l) reanalyses.*  
283

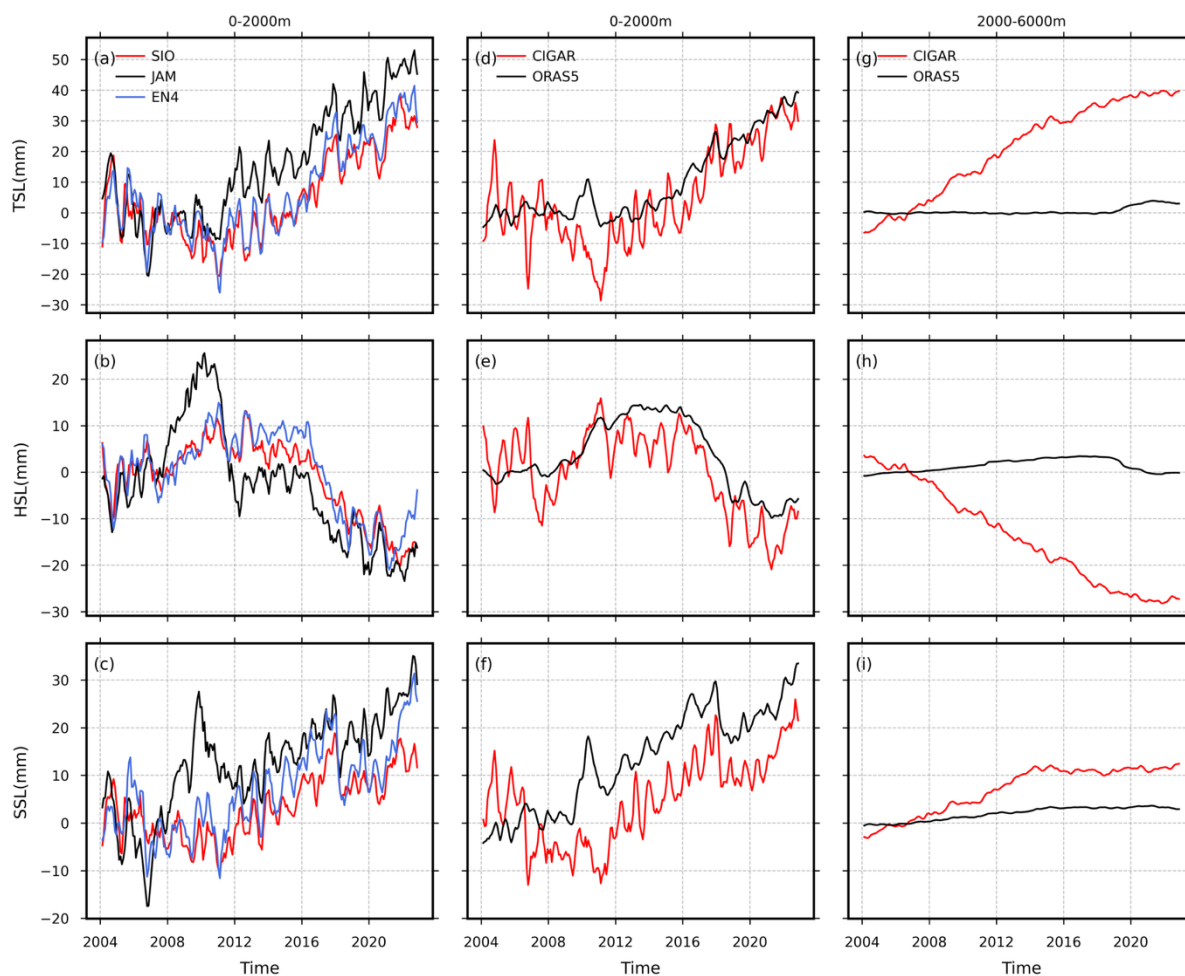
### 284 *3.2.2 Argo-based and ocean reanalysis thermosteric, halosteric and steric time series*

285 Next, we examine the thermosteric, halosteric and steric time series (weighted averages of the  
286 gridded data in the North Atlantic) for the different Argo and ocean reanalysis product (Figure  
287 4). Figure 4a,d indicate that the thermosteric component exhibits an upward trend in all  
288 products, although the rates of rise vary. Regarding the halosteric component (Figure 4b,e), we  
289 observe that the SIO and CIGAR products show a small decreasing trend that begins earlier  
290 than 2016, which may represent a true physical salinity increase during this early period.  
291 Among the three Argo products (Figure 4a-c), SIO and EN4 show strong agreement in  
292 thermosteric, halosteric, and steric sea level changes. In contrast, JAMSTEC deviates from the  
293 other two products, particularly in the halosteric component, which displays an unrealistic  
294 increase during the 2010s. Consequently, this discrepancy causes the total steric sea level  
295 change in JAMSTEC to mismatch with the other two products. In the following, we exclude  
296 the JAMSTEC product from the subsequent analysis.

297 Figure 4d-i presents the changes for CIGAR and ORAS5 in the upper 2000m ocean depth and  
298 from 2000m to 6000m (deep ocean). In the upper 2000m, Although there is a little difference  
299 in trend before 2010, they are consistent across components after 2010, although their  
300 amplitudes slightly differ. However, in the deep ocean (2000–6000m), substantial  
301 discrepancies exist between the two products. As mentioned above, ORAS5 exhibits a weak  
302 signal in the deep ocean; its thermosteric trend is nearly zero until 2019. In contrast, CIGAR  
303 shows a consistent and distinct upward trend. Regarding the halosteric change, ORAS5 shows  
304 a weakly rising trend until 2019, whereas CIGAR shows a consistent and obvious decrease.  
305 Finally, while both products exhibit rising trends in steric sea level change in the deep ocean,  
306 their magnitudes differ significantly. Given the unrealistically stationary thermosteric signal

307 observed in ORAS5 below 2000m, we suspect that this product is unreliable in its deep ocean  
308 variability.

309



310

311 *Figure 4. Time series of thermosteric (a, d, g), halosteric (b, e, h), and steric (c, f, i) sea level*  
312 *change in the North Atlantic. Panels (a–c) show the upper 2000 m derived from Argo products*  
313 *(SIO, JAM, EN4), while panels (d–i) are derived from CIGAR and ORAS5 reanalyses for the*  
314 *upper 2000 m (d–f) and the deep ocean 2000–6000 m (g–i). All time series have applied three-*  
315 *month moving average filtering. Global mean trend is included.*

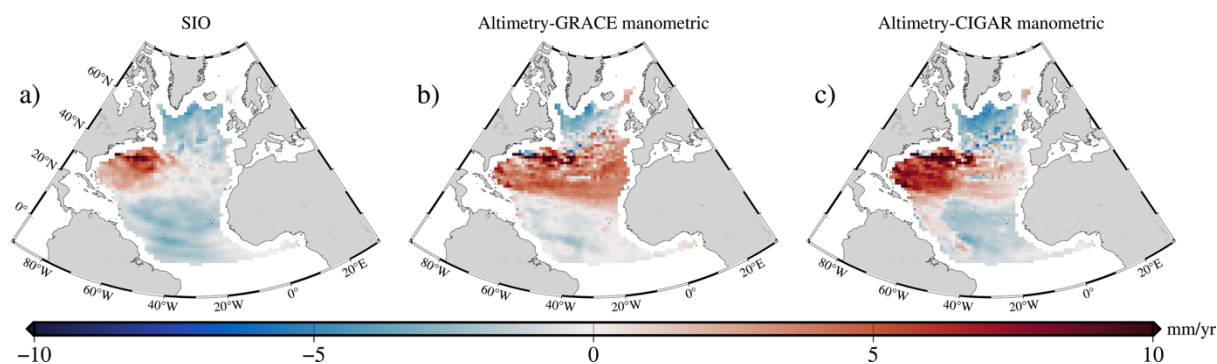


316 **3.3 Comparison between the SIO steric trends and altimetry sea level trends corrected for**  
317 **the manometric component**

318 In addition to directly obtaining the steric sea level trends, we can also derive it indirectly using  
319 the sea level budget equation (i.e., altimetry sea level minus manometric component computed  
320 at each grid mesh of the gridded products). In Figure 5, we compare the direct steric estimate  
321 from SIO with indirect estimates derived by subtracting different manometric products  
322 (GRACE or CIGAR) from altimetry trend data. It is important to note that the indirect method  
323 inherently includes deep ocean contribution and relies on independent observations.

324 From Figure 5, we clearly observe that the spatial trend pattern of SIO is more consistent with  
325 the “Altimetry minus CIGAR manometric” estimate, as both exhibit positive signals in the  
326 western North Atlantic. In contrast, the “Altimetry minus GRACE manometric” estimate  
327 displays a prominent positive signal in the eastern North Atlantic which is absent in the SIO  
328 data. This suggests that the GRACE manometric data contains substantial inaccuracies,  
329 particularly in the eastern North Atlantic, while “Altimetry minus CIGAR manometric” agrees  
330 rather well with the SIO steric trends.

331



332

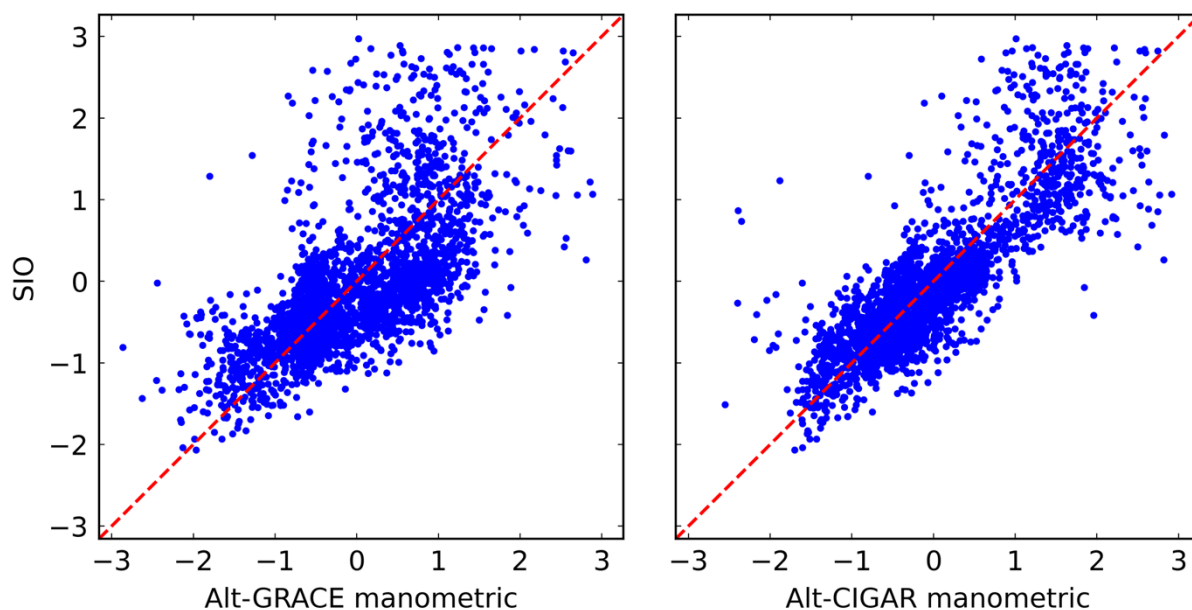
333 *Figure 5. Steric sea level trends derived directly from SIO and indirectly from Altimetry minus*  
334 *manometric estimates (GRACE or CIGAR).*

335



336 To highlight this further, Figure 6a, b shows the scatter plots between SIO gridpoint steric  
337 trends and “Altimetry minus GRACE manometric” and “Altimetry minus CIGAR manometric”  
338 grid point trends.

339 The scatter plots reveal distinct differences in the correlation between SIO observations and  
340 the two manometric estimates. In the negative SIO region (corresponding to the lower half of  
341 Figure 6 and the negative values regions in Figure 5), where most points align with the diagonal  
342 in both cases, the ‘Altimetry-CIGAR manometric’ points are clustered notably more tightly  
343 than those in the ‘Altimetry-GRACE manometric’ comparison. This indicates that in regions  
344 with negative steric sea level change, where both estimates correlate with SIO, the “Altimetry-  
345 CIGAR manometric” estimate maintains a higher spatial correlation compared to “Altimetry-  
346 GRACE manometric”. In the positive SIO areas (corresponding to the upper half of the plots),  
347 a portion of the data points in both estimates exhibit values lower than the SIO observations  
348 (indicated by points falling above the diagonal). However, this underestimation is much more  
349 pronounced for ‘Altimetry-GRACE manometric’, leading to a larger spread away from the  
350 diagonal compared to Altimetry-CIGAR manometric. This suggests that while the correlation  
351 with SIO decreases for both products in positive steric sea level trend regions (such as the  
352 western North Atlantic), the correlation of “Altimetry-GRACE” is notably weaker than that of  
353 “Altimetry-CIGAR manometric”.



354

355 *Figure 6. Scatter plots of SIO steric sea level change versus Altimetry minus manometric*  
356 *estimates (GRACE/left or CIGAR/right). The data have been normalized and outliers*  
357 *exceeding  $3\sigma$  were removed.*

358

### 359 **3.4 Residual trend maps in the North Atlantic**

360 In this section, we utilize data from the observing systems described above to compute spatial  
361 maps of the sea level budget residuals.

#### 362 *3.4.1 North Atlantic budget residuals of different manometric and steric (0-2000m)* 363 *components*

364 We computed the residuals by subtracting various combinations of manometric (GRACE,  
365 CIGAR) and steric (SIO, EN4, CIGAR, and ORAS5 upper 2000 m) components from the  
366 altimetry data (Figure 7).

367 As shown in Figure 7a,e, the resulting residuals implicitly include a deep ocean steric  
368 contribution, which is not accounted for since the steric data are limited here to the upper 2000



369 m. This is consistent with previous results from Bouih et al. (2025), who observed positive  
370 residuals in the North Atlantic for both manometric cases., Similarly positive residuals are  
371 found in the eastern North Atlantic for the GRACE manometric component and in the western  
372 North Atlantic for the CIGAR manometric component.

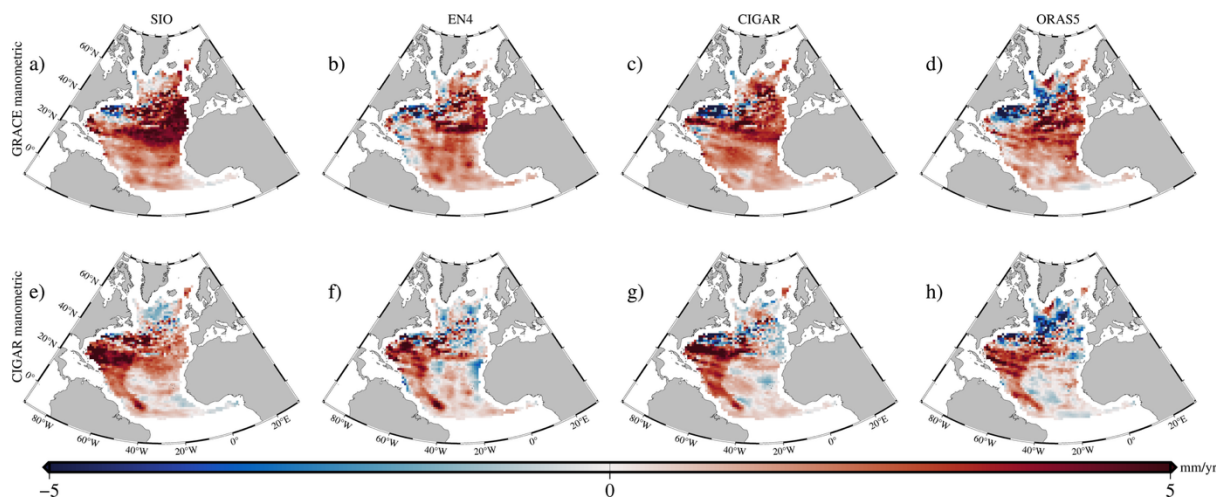
373 From Figure 7, we also observe that the spatial distribution of the residuals remains similar  
374 when the manometric component is held fixed while varying the steric components. However,  
375 the residual magnitude is different. Specifically, when using the GRACE manometric  
376 component, the positive signal derived from SIO is stronger in the eastern North Atlantic  
377 compared to other steric products. When using the CIGAR manometric component, the  
378 positive signals from SIO and CIGAR are stronger in the western North Atlantic compared to  
379 EN4 and ORAS5.

380 To quantify the residuals, we computed the latitude-weighted spatial mean trend of each map.  
381 Results are shown in Table 1 (remind that results in Table 1 do not account for the global mean  
382 trends). From Table 1, we observe that regardless of the steric data used (whether from Argo  
383 or ocean reanalyses), the residuals derived using the CIGAR manometric component are  
384 always smaller than those derived using GRACE. Furthermore, for a given manometric  
385 component, the residual with SIO is larger than that with EN4, even though SIO has corrected



386 for the salinity drift since 2016. Besides, the residual with CIGAR steric is larger than that with  
 387 ORAS5.

388



389

390 *Figure 7. Maps of sea level residuals in the North Atlantic. The residuals are calculated by*  
 391 *subtracting manometric and steric components from satellite altimetry. The manometric*  
 392 *component is derived from GRACE (a–d) and CIGAR (e–h). These are combined with upper*  
 393 *2000 m steric estimates from SIO (a, e), EN4 (b, f), CIGAR (c, g), and ORAS5 (d, h).*

394

395

396 *Table 1. Trend values (mm/yr) of sea level residuals in the North Atlantic corresponding to*  
 397 *different steric products (0–2000m) and the two manometric components. Global mean trends*  
 398 *were removed. Uncertainties are 2-sigma errors of the least-squares fit.*

399

Trend (mm/yr)	SIO	EN4	CIGAR	ORAS5
GRACE manometric	2.15±0.19	1.43±0.22	1.52±0.21	1.10±0.20
CIGAR manometric	1.50±0.23	0.77±0.23	0.86±0.25	0.45±0.16

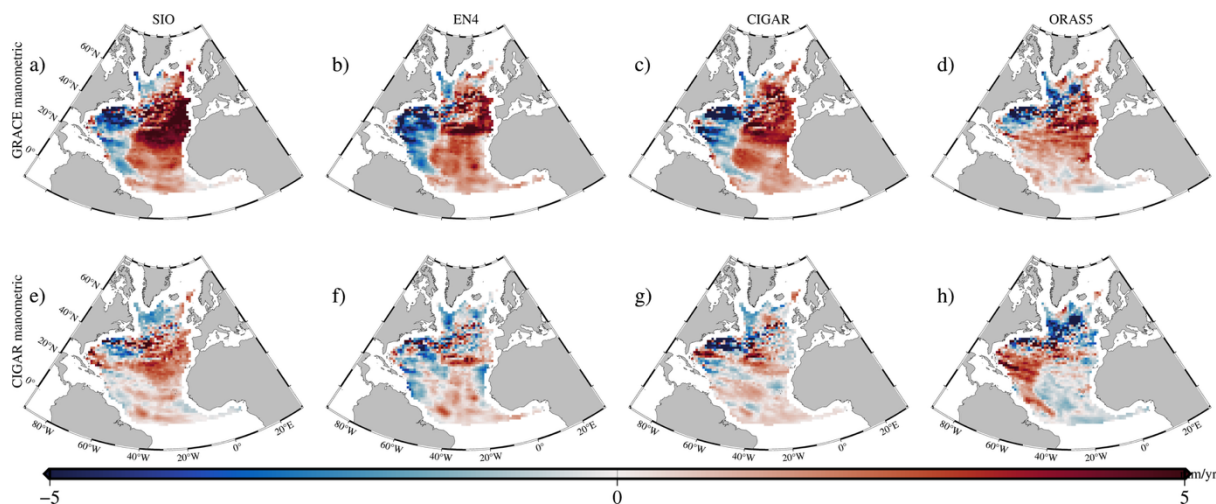
400



401 *3.4.2 North Atlantic budget residuals and deep ocean steric contribution*

402 In this section, we added the deep ocean steric sea level change to the upper 2000 m steric  
403 estimates, considering both the CIGAR and ORAS5 deep steric data, and using either GRACE  
404 or CIGAR for the manometric components. Resulting residual trends are shown in Figure 8 .  
405 For all cases except the ORAS5 deep ocean case, the residuals derived using GRACE  
406 manometric data (Figure 8a–c) show a dipole pattern (positive in the east, negative in the west)  
407 compared to the results without the deep ocean component (Figure 7). Table 2 summarizes the  
408 residual trend values for all cases (as for Table 1, remind that results in Table 2 do not account  
409 for the global mean trends). Comparing results from Table 1 and Table 2, we note that the mean  
410 residual magnitude is significantly reduced when the deep ocean steric change is included: by  
411 ~30% when using GRACE for the manometric component and SIO for the upper 0–2000m  
412 steric sea level, and by ~50% when using CIGAR for both the steric (full depth and manometric  
413 component). Based on CIGAR, the deep steric contribution to the North Atlantic sea level  
414 budget (in addition to the global mean deep ocean contribution) amounts to  $0.62 \pm 0.04$  mm/yr.  
415 In contrast, when using the CIGAR manometric component (Figure 8e–h), the residuals  
416 decrease significantly in both spatial variability and magnitude. Notably, the sea level budget  
417 is effectively nearly closed within error bars when combining CIGAR manometric and CIGAR  
418 steric data. Finally, it is worth noting that for SIO, positive residuals are observed in the eastern  
419 North Atlantic regardless of whether GRACE or CIGAR manometric data is used.

420



421

422 *Figure 8. Maps of sea level residuals in the North Atlantic, calculated as in Figure 7 but with*  
 423 *the inclusion of the deep ocean (below 2000 m) steric component. The deep ocean contribution*  
 424 *is derived from CIGAR for panels (a–c, e–g) and from ORAS5 for panels (d, h). In panels a–c,*  
 425 *the manometric component is from GRACE while it is from CIGAR in panels e–h.*

426

427 *Table 2. Trend values (mm/yr) of sea level residuals in the North Atlantic for four steric*  
 428 *products and two manometric components. For SIO and EN4, the deep ocean contribution*  
 429 *from CIGAR is added. For CIGAR and ORAS5, their own deep steric contributions are*  
 430 *considered. Global mean trends removed. Uncertainties are 2-sigma errors of the least-*  
 431 *squares fit.*

432

Trend (mm/yr)	SIO	EN4	CIGAR	ORAS5
GRACE manometric	$1.53 \pm 0.21$	$0.81 \pm 0.24$	$0.90 \pm 0.23$	$0.87 \pm 0.20$
CIGAR manometric	$0.88 \pm 0.20$	$0.15 \pm 0.21$	$0.24 \pm 0.22$	$0.22 \pm 0.15$

### 433 3.5 Time series of the North Atlantic mean sea level budget

434 Based on the analysis above, the deep ocean contribution to the North Atlantic sea level budget  
 435 cannot be ignored. To assess the influence of the deep ocean on the sea level budget, we



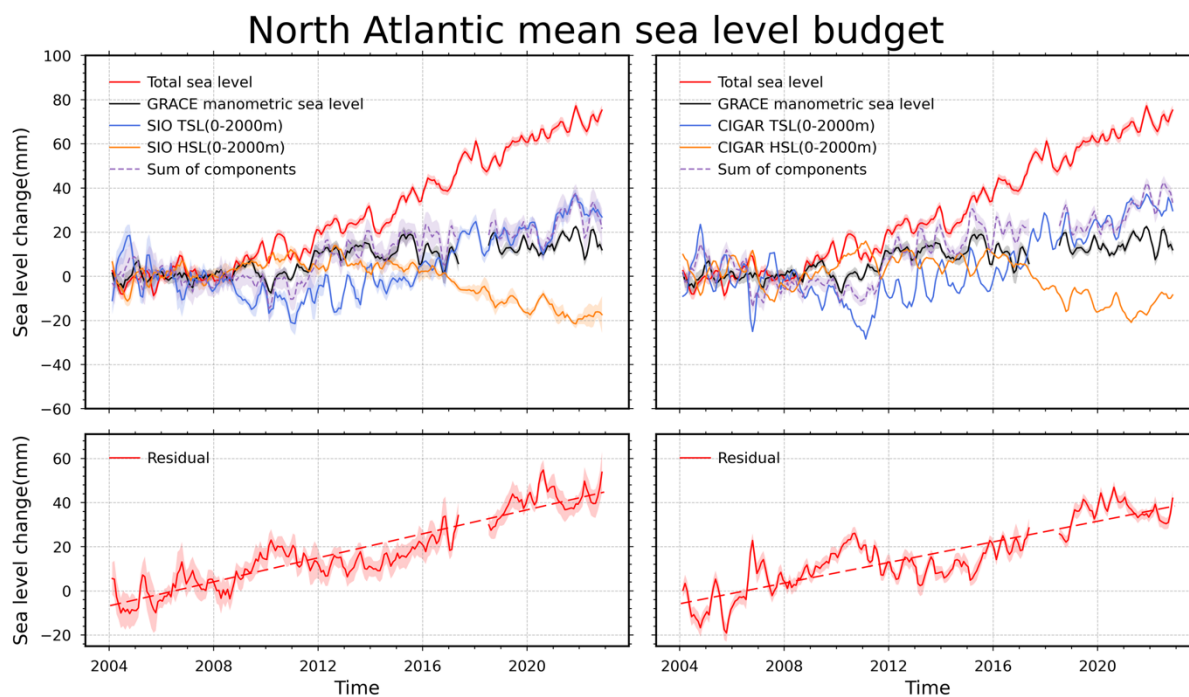
436 computed time series for each component, including total sea level, manometric sea level,  
437 thermosteric sea level, and halosteric sea level. Compared to results discussed above, here we  
438 account for the global mean trend of each component.

439 *3.5.1 North Atlantic mean sea level budget time series without deep ocean (global mean trends*  
440 *included)*

441 Here, we have reintroduced the global mean trend of each component. Since the CIGAR  
442 manometric component does not fully account for the external sea water mass addition to the  
443 ocean due to land ice melt and terrestrial waters, we adopt GRACE data to represent the total  
444 manometric sea level change (i.e., global mean trend accounted for). Regarding the steric sea  
445 level component, we selected the SIO product for Argo estimates, as it corrects for the salinity  
446 drift. For ocean reanalyses, we only consider the CIGAR reanalysis.

447 Figure 9 presents the sea level budget time series (global mean trends accounted for) in the  
448 North Atlantic without the deep ocean steric sea level change. Residual time series are also  
449 shown. The left/right panels use SIO/CIGAR steric sea level change in upper 2000m.  
450 Comparing Figure 9 left and right panels, we observe that the halosteric components from SIO  
451 and CIGAR slightly differ. For SIO, a slight halosteric decrease is observed over 2012-2015,  
452 with a linear trend of  $-1.10 \pm 0.94$  mm/yr during the such period, then it increases to  $-3.20 \pm 0.9$   
453 mm/yr over 2016-2022. Consequently, the SIO halosteric trend over 2012-2022 amounts to -  
454  $2.87 \pm 0.21$  mm/yr. In terms of global mean trend, the SIO halosteric time series does not show  
455 any trend (as expected since the salinity drift is supposed to be corrected). Thus, the SIO  
456 halosteric decrease observed in the North Atlantic may possibly reflect a truly physical salinity  
457 increase. As of 2016, the CIGAR halosteric decrease is slightly larger than for SIO, possibly a  
458 consequence of the salinity drift error not corrected for in the assimilated EN4 salinity data.  
459 The mean residual trends amount to  $2.72 \pm 0.19$  mm/yr and  $2.34 \pm 0.21$  mm/yr for the SIO and  
460 CIGAR steric cases respectively, i.e., not significantly different.

461



462

463 *Figure 9. Time series of North Atlantic sea level components (top) and residuals (bottom) for*  
464 *the upper 2000m. The analysis uses Altimetry and GRACE manometric data, combined with*  
465 *steric estimates from SIO (left) and CIGAR (right). All time series have applied three-month*  
466 *moving average filtering. The global mean trend of each component is included.*

467

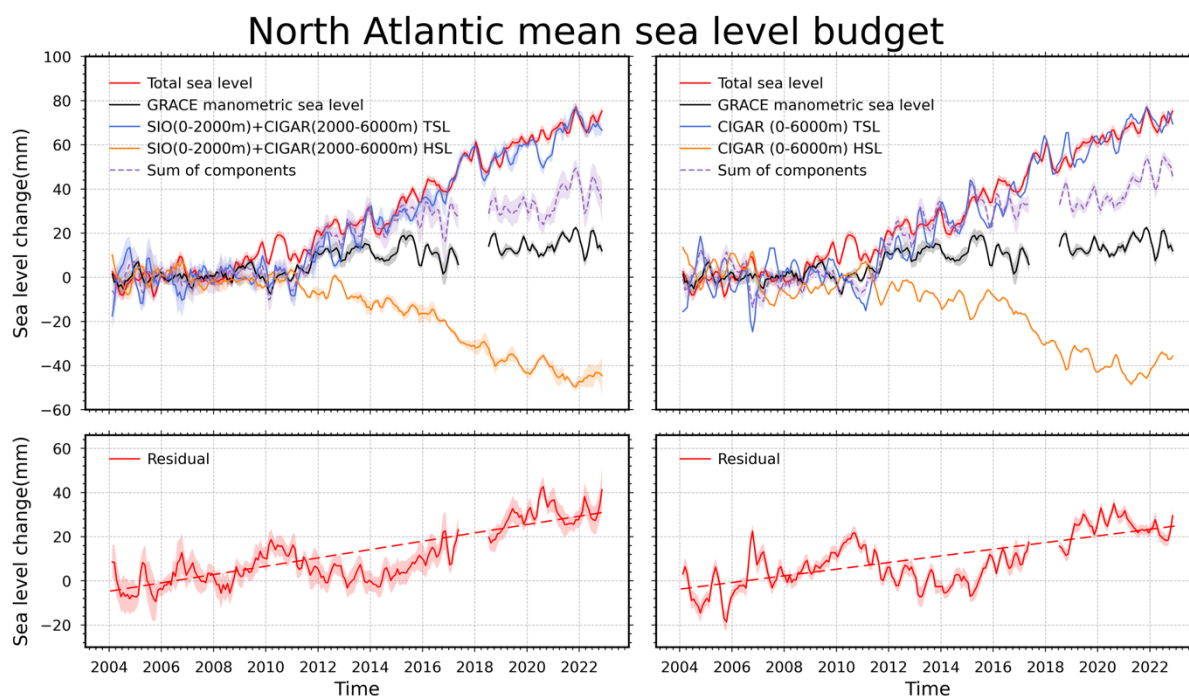
468 *3.5.2 North Atlantic sea level budget time series with the deep ocean contribution (global mean*  
469 *trends included)*

470 In this section, we add the deep ocean contribution from the CIGAR reanalysis. As in section  
471 3.5.1, the GRACE manometric component is considered, and for the upper 2000m steric  
472 component, both SIO and CIGAR data are used. The corresponding sea level budget time series  
473 for the North Atlantic are shown in Figure 10.

474 As illustrated in Figure 10, with the inclusion of the deep ocean contribution, the halosteric  
475 decline in both panels become more evident compared to the case without the deep ocean.



476 Specifically, the CIGAR component also shows a slight decrease starting in 2012. However,  
477 unlike the SIO trend, which maintains a relatively stable decline throughout the study time span,  
478 the CIGAR decrease still exhibits a sudden intensification after 2016. Similarly, the  
479 thermosteric sea level also displays a stronger increasing trend compared to the case without  
480 the deep ocean.  
481 Consequently, the total steric sea level trend is larger than in the case without the deep ocean  
482 contribution. Finally, the inclusion of the deep ocean contribution leads to a reduction in the  
483 North Atlantic residual trends for both cases: for the estimate based on SIO (upper 2000 m),  
484 the trend decreases by about 30%, from  $2.72 \pm 0.19$  mm/yr to  $1.89 \pm 0.21$  mm/yr, whereas for  
485 the estimate based on CIGAR, it drops from  $2.34 \pm 0.21$  mm/yr to  $1.51 \pm 0.23$  mm/yr.  
486



487  
488 *Figure 10. Time series of North Atlantic sea level change components (top) and budget*  
489 *residuals (bottom). The left panels use a hybrid steric estimate (SIO for 0–2000m combined*



490 *with CIGAR for 2000–6000m), while the right panels use the full-depth CIGAR steric estimate*  
491 *(0–6000m). In both cases, Altimetry and GRACE manometric data are used. All time series*  
492 *have applied three-month moving average filtering. The global mean trend of each component*  
493 *is included.*

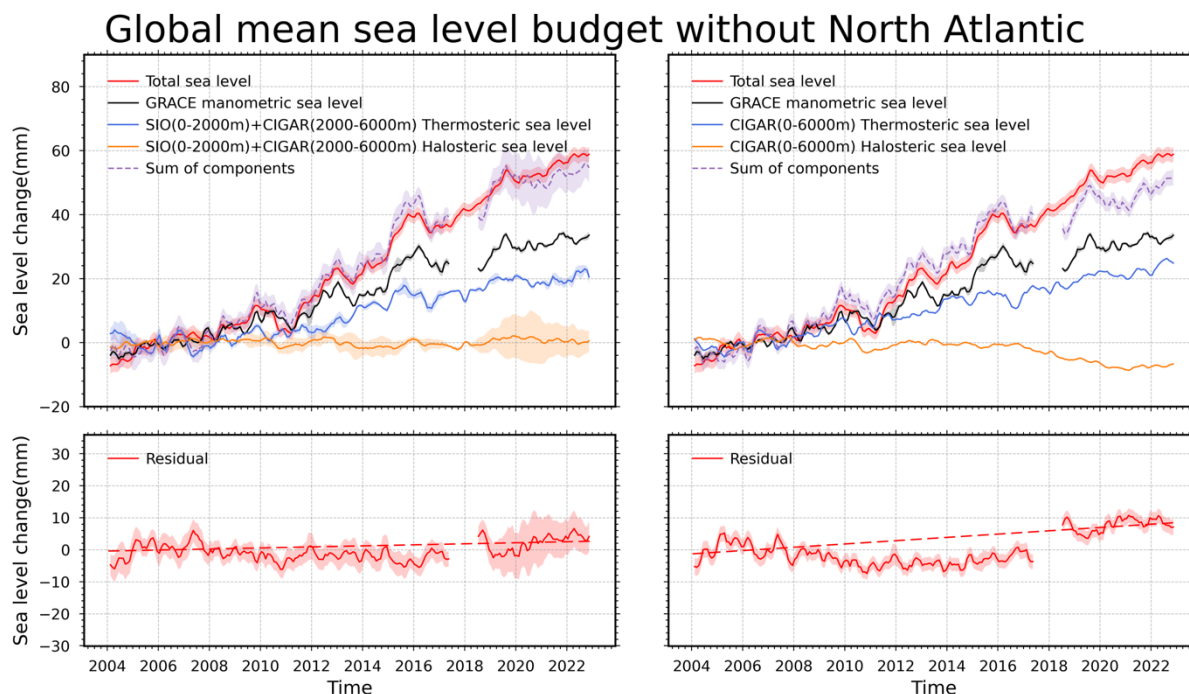
494

495 *3.5.3 Sea level budget of all oceans but without the North Atlantic Ocean, with the deep ocean*  
496 *contribution added*

497 In Bouih et al. (2025)’s study, the sea level budget for the global ocean excluding the North  
498 Atlantic (without the deep ocean steric contribution) was not closed. In this section, we  
499 consider the deep ocean steric sea level change contribution to the sea level budget. We  
500 compute the sea level budget for the global ocean excluding the North Atlantic using the same  
501 data products as in Section 3.5.2. The corresponding results are shown in Figure 11.

502 In the left panel (using SIO data for the upper 2000 m), we observe that the halosteric sea level  
503 change is nearly zero. The residual is very small, estimated at  $0.16 \pm 0.08$  mm/yr. Thus,  
504 considering the whole oceanic domain without the North Atlantic, the sea level budget is closed  
505 when SIO data are used for the upper 2000 m ocean layer. In contrast, the right panel (using  
506 CIGAR data for all depths) shows a distinct decrease in halosteric sea level starting in 2016,  
507 due to the assimilation of EN4 data in CIGAR (not corrected for the salinity drift).  
508 Nevertheless, the residual trend of the right panel is small ( $0.51 \pm 0.11$  mm/yr), suggesting quasi  
509 closure of the sea level budget.

510



511

512 *Figure 11. Time series of sea level components (top) and residuals (bottom) for the global*  
513 *ocean excluding the North Atlantic. The left panels use a hybrid steric estimate (SIO for 0–*  
514 *2000 m combined with CIGAR for 2000–6000m), while the right panels use the full-depth*  
515 *CIGAR estimate (0–6000m). All time series have applied three-month moving average filtering.*  
516 *The global mean trend of each component is included.*

517

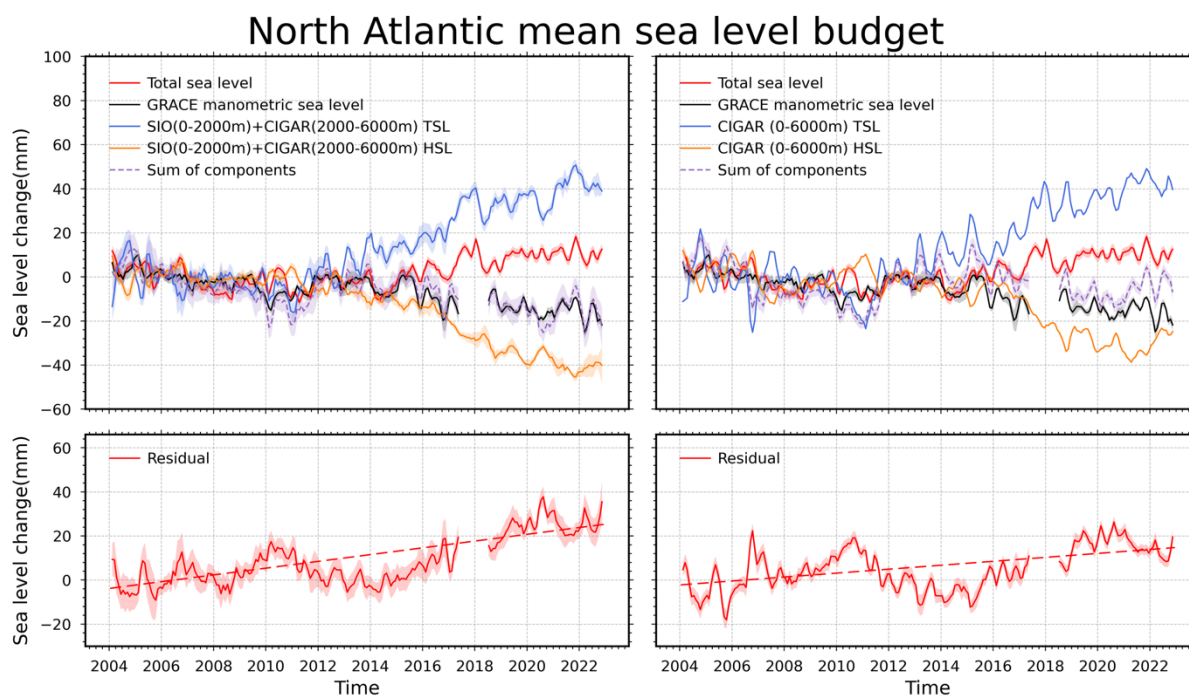
518 *3.5.4 North Atlantic sea level budget time series with the deep ocean contribution (global mean*  
519 *trends removed)*

520 Here, we compute the North Atlantic sea level budget (including the deep ocean contribution)  
521 with the global mean sea level trends of all components removed. The objective is to determine  
522 which part of the non-closure in the North Atlantic budget may result from errors in the regional  
523 components (i.e., independently from errors in the global mean trends). Figure 12 presents the  
524 budget time series using GRACE for the manometric component. We consider two steric cases:  
525 the hybrid case (SIO 0–2000 m plus CIGAR deep ocean) and the CIGAR full-depth case.



526 The mean residual trends are estimated at  $1.53 \pm 0.21$  mm/yr for the hybrid steric case and  
527  $0.88 \pm 0.20$  mm/yr for the CIGAR full-depth case. Comparing these results (where global mean  
528 trends are removed) with those in Figure 10 (where global mean trends are included), we  
529 observe very little difference in the mean residual trends. This suggests that errors in the global  
530 mean trends are small, and that the reported residuals in the North Atlantic budget are primarily  
531 driven by component errors at the regional scale.

532



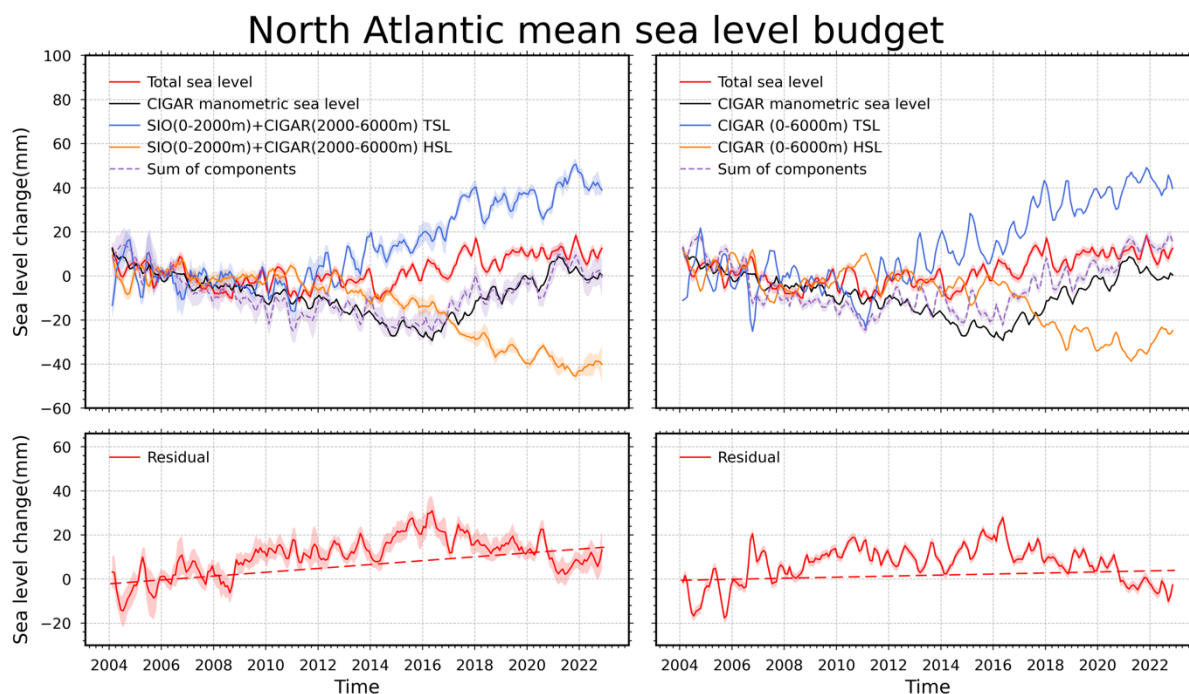
533

534 *Figure 12. Time series of North Atlantic sea level change components (top) and budget*  
535 *residuals (bottom). The left panels use a hybrid steric estimate (SIO for 0–2000m combined*  
536 *with CIGAR for 2000–6000m), while the right panels use the full-depth CIGAR steric estimate*  
537 *(0–6000m). In both left and right panels, GRACE manometric components are considered. All*  
538 *time series have applied three-month moving average filtering. The global mean trend of each*  
539 *component is removed.*

540



541 Figure 13 displays the corresponding budget time series using CIGAR for the manometric  
542 component. Similarly, we evaluate the residuals for both steric configurations. When using the  
543 CIGAR manometric data, the mean residual trends amount to  $0.88 \pm 0.20$  mm/yr for the hybrid  
544 steric case (SIO 0–2000 m plus CIGAR deep ocean) and  $0.24 \pm 0.22$  mm/yr for the CIGAR full-  
545 depth case.  
546



547

548 *Figure 13. Time series of North Atlantic sea level change components (top) and budget*  
549 *residuals (bottom). The left panels use a hybrid steric estimate (SIO for 0–2000m combined*  
550 *with CIGAR for 2000–6000m), while the right panels use the full-depth CIGAR steric estimate*  
551 *(0–6000m). In both left and right panels, CIGAR manometric components are considered. All*  
552 *time series have applied three-month moving average filtering. The global mean trend of each*  
553 *component is removed.*  
554

555 Comparing the results from Figure 12 and Figure 13, we note that using CIGAR for the  
556 manometric component consistently leads to smaller regional residuals than using GRACE,



557 regardless of the steric product considered. It is worth noting that the configuration using  
558 CIGAR for both manometric and steric components yields a mean residual trend of  $0.24 \pm 0.22$   
559 mm/yr, nearly four times smaller than in the case where the GRACE manometric component  
560 is used ( $0.90 \pm 0.23$  mm/yr). These results confirm our previous conclusions based on the  
561 residual trend maps.

562 In Table 3, the mean North Atlantic residual trends presented in Figure 9, 12 and 13 are  
563 quantified.

564

565 *Table 3. Mean North Atlantic residual trends (mm/yr) for different products of the sea level*  
566 *budget.*

Trends(mm/yr)	GRACE manometric (GMSL trend added)	GRACE manometric (GMSL trend removed)	CIGAR manometric (GMSL trend removed)
SIO (0-2000m) +Deep Ocean	$1.89 \pm 0.21$	$1.53 \pm 0.21$	$0.88 \pm 0.20$
CIGAR (Full depth)	$1.51 \pm 0.23$	$0.90 \pm 0.23$	$0.24 \pm 0.22$

567

## 568 **4 Discussion**

569 In this study, we have revisited the sea level budget of the North Atlantic over the 2004-2022  
570 period, using a variety of different data sets. The objective was to further investigate the results  
571 from Bouih et al. (2025) who reported non-closure of the sea level budget in the North Atlantic  
572 over the same time span, and to identify which components of the budget (or which missing  
573 component) are responsible.

574 The main results of our study can be summarized as follows:



- 575 (1) By comparing the SIO-based steric sea level with “Altimetry minus manometric sea  
576 level” in two cases (GRACE and CIGAR-based manometric component) over the North  
577 Atlantic, the use of CIGAR manometric sea level provides higher correlation than when  
578 using GRACE. This comparison indicates potential errors in the GRACE and GRACE-  
579 FO data, particularly in the eastern region of the North Atlantic basin where the  
580 manometric component is strongly negative. The cause is so far unknown but possibly  
581 related to the correction applied to GRACE data, e.g., the geocenter or GIA corrections.  
582 These needs dedicated investigation.
- 583 (2) As of 2012, a decreasing trend is observed in the SIO halosteric component which  
584 suggests a physically real increase in salinity of the North Atlantic. Again, this needs  
585 further investigation.
- 586 (3) Our study shows that the deep ocean (>2000 m of depth) contribution to the North  
587 Atlantic sea level budget is not negligible and needs to be taken into account to obtain  
588 better closure of the sea level budget in this region. Based on CIGAR, the additional  
589 deep ocean steric contribution (above the global mean deep ocean contribution) to the  
590 North Atlantic sea level budget amounts to  $0.62 \pm 0.04$  mm/yr.
- 591 (4) Accounting for the deep ocean steric contribution reduces by a factor of 30% the  
592 residuals of the North Atlantic sea level budget when using the GRACE manometric  
593 component, and by a factor of two when using CIGAR for the manometric component  
594 (and CIGAR full depth for the steric component). In the latter case, the mean residual  
595 trend over the North Atlantic is <1mm/yr, i.e., of the same order of magnitude as the  
596 regional trend error for altimetry gridded data according to Prandi et al. (2021). We can  
597 thus conclude that the closure of the sea level budget holds within the data uncertainties  
598 in this case.



599 (5) Our results also indicate that the main contribution to the mean North Atlantic residual  
600 trend comes from errors on the regional components (whatever the products used for  
601 the components) rather than from errors in the global mean trends.

602 (6) The North Atlantic sea level budget is closed within data uncertainties when using the  
603 CIGAR reanalysis for both the manometric and steric components.

604 (7) Our study also shows that the sea level budget of all other oceans (North Atlantic  
605 excluded) is almost closed when accounting for the deep ocean steric contribution based  
606 on the CIGAR ocean reanalysis

607 These new findings represent a step further towards better understanding of the present-day sea  
608 level budget in the North Atlantic region. Those investigations also support the need to better  
609 observe the deep ocean especially in the North Atlantic Ocean which is one of the objectives  
610 of the One Argo Project (Thierry et al., 2025). Nevertheless, some issues still merit deeper  
611 investigation. We can quote the followings, among others: Why GRACE manometric data give  
612 less good results in the North Atlantic than the CIGAR-based manometric sea level? Which  
613 inaccurate correction applied to GRACE is involved? Is it related to the GIA or the geocenter  
614 corrections applied to GRACE? What causes the slight salinity increase observed in the North  
615 Atlantic (full depth) with SIO data? Can we explain the physical process causing the reported  
616 CIGAR-based positive deep ocean steric sea level? What is the impact on the CIGAR steric  
617 component estimates of the use of EN4 (with no salinity drift correction applied) in the  
618 assimilation procedure? What is the source of the (small) remaining residual trend of the North  
619 Atlantic sea level budget (after accounting for the deep ocean)? Clearly, future studies should  
620 be devoted to try answering these puzzling questions.

621



622 **Author contributions**

623 AC, WL and ZS designed the study. All analyses have been performed by ZS. ZS and AC  
624 wrote a first version of the manuscript. All co-authors contributed to the discussion of the  
625 results, editing and final writing of the manuscript.

626

627 **Competing interests**

628 The contact author has declared that none of the authors has any competing interests.

629

630 **Acknowledgements**

631 Zhe Song is supported by China Scholarship Council. This study is a contribution to the  
632 ongoing ESA (European Space Agency) CCI (Climate Change Initiative) project entitled ‘Sea  
633 level budget closure CCI+ (SLBC\_CCI+)’. This work is a contribution to the GREAT project  
634 funded by CNES through the Ocean Surface Topography Science Team (OSTST).

635



## 636 **References**

- 637 Adhikari, S., Ivins, E. R., Frederikse, T., Landerer, F. W., and Caron, L.: Sea-level fingerprints  
638 emergent from GRACE mission data, *Earth System Science Data*, 11, 629–646,  
639 <https://doi.org/10.5194/essd-11-629-2019>, 2019.
- 640 Barnoud, A., Pfeffer, J., Guérou, A., Frery, M., Siméon, M., Cazenave, A., Chen, J., Llovel,  
641 W., Thierry, V., Legeais, J., and Ablain, M.: Contributions of Altimetry and Argo to Non-  
642 Closure of the Global Mean Sea Level Budget Since 2016, *Geophysical Research Letters*, 48,  
643 <https://doi.org/10.1029/2021gl092824>, 2021.
- 644 Bouih, M., Barnoud, A., Yang, C., Storto, A., Blazquez, A., Llovel, W., Fraudeau, R., and  
645 Cazenave, A.: Regional sea level trend budget over 2004–2022, *Ocean Sci.*, 21, 1425–1440,  
646 <https://doi.org/10.5194/os-21-1425-2025>, 2025.
- 647 Brown, S., Willis, J., and Fournier, S.: Jason-3 Wet Path Delay Correction,  
648 <https://doi.org/10.5067/J3L2G-PDCOR>, 2023.
- 649 Camargo, C. M. L., Riva, R. E. M., Hermans, T. H. J., Schütt, E. M., Marcos, M., Hernandez-  
650 Carrasco, I., and Slangen, A. B. A.: Regionalizing the sea-level budget with machine learning  
651 techniques, *Ocean Science*, 19, 17–41, <https://doi.org/10.5194/os-19-17-2023>, 2023.
- 652 Chen, J., Tapley, B., Seo, K., Wilson, C., and Ries, J.: Improved Quantification of Global Mean  
653 Ocean Mass Change Using GRACE Satellite Gravimetry Measurements, *Geophys. Res. Lett.*,  
654 46, 13984–13991, <https://doi.org/10.1029/2019GL085519>, 2019.
- 655 Chen, J., Tapley, B., Wilson, C., Cazenave, A., Seo, K.-W., and Kim, J.-S.: Global Ocean Mass  
656 Change From GRACE and GRACE Follow-On and Altimeter and Argo Measurements,  
657 *Geophysical Research Letters*, 47, e2020GL090656, <https://doi.org/10.1029/2020GL090656>,  
658 2020.
- 659 Cheng, L., Zhu, J., Cowley, R., Boyer, T., and Wijffels, S.: Time, Probe Type, and Temperature  
660 Variable Bias Corrections to Historical Expendable Bathythermograph Observations, *Journal*



661 of Atmospheric and Oceanic Technology, 31, 1793–1825, <https://doi.org/10.1175/JTECH-D->  
662 13-00197.1, 2014.

663 Dieng, H. B., Cazenave, A., Meyssignac, B., and Ablain, M.: New estimate of the current rate  
664 of sea level rise from a sea level budget approach, *Geophysical Research Letters*, 44, 3744–  
665 3751, <https://doi.org/10.1002/2017GL073308>, 2017.

666 Dobslaw, H., Bergmann-Wolf, I., Dill, R., Poropat, L., Thomas, M., Dahle, C., Esselborn, S.,  
667 König, R., and Flechtner, F.: A new high-resolution model of non-tidal atmosphere and ocean  
668 mass variability for de-aliasing of satellite gravity observations: AOD1B RL06, *Geophysical*  
669 *Journal International*, 211, 263–269, <https://doi.org/10.1093/gji/ggx302>, 2017.

670 Flechtner, F., Dobslaw, H., and Fagiolini, E.: GRACE AOD1B product description document  
671 for product release 05, 2014.

672 Frederikse, T., Riva, R., Kleinherenbrink, M., Wada, Y., van den Broeke, M., and Marzeion,  
673 B.: Closing the sea level budget on a regional scale: Trends and variability on the Northwestern  
674 European continental shelf, *Geophysical Research Letters*, 43, 10,864–10,872,  
675 <https://doi.org/10.1002/2016GL070750>, 2016.

676 Gregory, J. M., Griffies, S. M., Hughes, C. W., Lowe, J. A., Church, J. A., Fukimori, I., Gomez,  
677 N., Kopp, R. E., Landerer, F., Cozannet, G. L., Ponte, R. M., Stammer, D., Tamisiea, M. E.,  
678 and van de Wal, R. S. W.: Concepts and Terminology for Sea Level: Mean, Variability and  
679 Change, Both Local and Global, *Surv Geophys*, 40, 1251–1289,  
680 <https://doi.org/10.1007/s10712-019-09525-z>, 2019.

681 Hamlington, B. D., Gardner, A. S., Ivins, E., Lenaerts, J. T. M., Reager, J. T., Trossman, D. S.,  
682 Zaron, E. D., Adhikari, S., Arendt, A., Aschwanden, A., Beckley, B. D., Bekaert, D. P. S.,  
683 Blewitt, G., Caron, L., Chambers, D. P., Chandanpurkar, H. A., Christianson, K., Csatho, B.,  
684 Cullather, R. I., DeConto, R. M., Fasullo, J. T., Frederikse, T., Freymueller, J. T., Gilford, D.  
685 M., Giroto, M., Hammond, W. C., Hock, R., Holschuh, N., Kopp, R. E., Landerer, F., Larour,  
686 E., Menemenlis, D., Merrifield, M., Mitrovica, J. X., Nerem, R. S., Nias, I. J., Nieves, V.,



687 Nowicki, S., Pangaluru, K., Piecuch, C. G., Ray, R. D., Rounce, D. R., Schlegel, N.-J.,  
688 Seroussi, H., Shirzaei, M., Sweet, W. V., Velicogna, I., Vinogradova, N., Wahl, T., Wiese, D.  
689 N., and Willis, M. J.: Understanding of Contemporary Regional Sea-Level Change and the  
690 Implications for the Future, *Reviews of Geophysics*, 58, e2019RG000672,  
691 <https://doi.org/10.1029/2019RG000672>, 2020.

692 Horwath, M., Gutknecht, B. D., Cazenave, A., Palanisamy, H. K., Marti, F., Marzeion, B.,  
693 Paul, F., Le Bris, R., Hogg, A. E., Otsuka, I., Shepherd, A., Döll, P., Cáceres, D., Müller  
694 Schmied, H., Johannessen, J. A., Nilsen, J. E. Ø., Raj, R. P., Forsberg, R., Sandberg Sørensen,  
695 L., Barletta, V. R., Simonsen, S. B., Knudsen, P., Andersen, O. B., Rannald, H., Rose, S. K.,  
696 Merchant, C. J., Macintosh, C. R., von Schuckmann, K., Novotny, K., Groh, A., Restano, M.,  
697 and Benveniste, J.: Global sea-level budget and ocean-mass budget, with a focus on advanced  
698 data products and uncertainty characterisation, *Earth System Science Data*, 14, 411–447,  
699 <https://doi.org/10.5194/essd-14-411-2022>, 2022.

700 Liu, C., Liang, X., Chambers, D., and Ponte, R.: Global Patterns of Spatial and Temporal  
701 Variability in Salinity from Multiple Gridded Argo Products, *Journal of Climate*,  
702 <https://doi.org/10.1175/JCLI-D-20-0053.1>, 2020.

703 Llovel, W. and Hochet, A.: Salinity Contribution to Regional Sea Level Trends in the Tropical  
704 Southwestern Pacific Ocean Over 2014–2023, *Geophysical Research Letters*, 52,  
705 e2025GL116115, <https://doi.org/10.1029/2025GL116115>, 2025.

706 Llovel, W., Balem, K., Tajouri, S., and Hochet, A.: Cause of Substantial Global Mean Sea  
707 Level Rise Over 2014–2016, *Geophysical Research Letters*, 50, e2023GL104709,  
708 <https://doi.org/10.1029/2023GL104709>, 2023.

709 McDougall, T. J., Barker, P. M., Marine, CSIRO., and Research, A.: Getting started with  
710 TEOS-10 and the gibbs seawater (GSW) oceanographic toolbox, Trevor J. McDougall, 2011.



- 711 Mu, D., Church, J. A., King, M., Ludwigsen, C. B., and Xu, T.: Contrasting Discrepancy in the  
712 Sea Level Budget Between the North and South Atlantic Ocean Since 2016, *Earth and Space*  
713 *Science*, 11, e2023EA003133, <https://doi.org/10.1029/2023EA003133>, 2024.
- 714 Nerem, R. S., Beckley, B. D., Fasullo, J. T., Hamlington, B. D., Masters, D., and Mitchum, G.  
715 T.: Climate-change–driven accelerated sea-level rise detected in the altimeter era, *Proceedings*  
716 *of the National Academy of Sciences*, 115, 2022–2025,  
717 <https://doi.org/10.1073/pnas.1717312115>, 2018.
- 718 Pardaens, A. K., Gregory, J. M., and Lowe, J. A.: A model study of factors influencing  
719 projected changes in regional sea level over the twenty-first century, *Clim Dyn*, 36, 2015–2033,  
720 <https://doi.org/10.1007/s00382-009-0738-x>, 2011.
- 721 Peltier, W. R., Argus, D. F., and Drummond, R.: Comment on “An Assessment of the ICE-  
722 6G\_C (VM5a) Glacial Isostatic Adjustment Model” by Purcell et al.: The ICE-6G\_C (VM5a)  
723 GIA model, *J. Geophys. Res. Solid Earth*, 123, 2019–2028,  
724 <https://doi.org/10.1002/2016JB013844>, 2018.
- 725 Ponte, R. M., Sun, Q., Liu, C., and Liang, X.: How Salty Is the Global Ocean: Weighing It All  
726 or Tasting It a Sip at a Time?, *Geophysical Research Letters*, 48, e2021GL092935,  
727 <https://doi.org/10.1029/2021GL092935>, 2021.
- 728 Roemmich, D. and Gilson, J.: The 2004–2008 mean and annual cycle of temperature, salinity,  
729 and steric height in the global ocean from the Argo Program, *Progress in Oceanography*, 82,  
730 81–100, <https://doi.org/10.1016/j.pocean.2009.03.004>, 2009.
- 731 Royston, S., Dutt Vishwakarma, B., Westaway, R., Rougier, J., Sha, Z., and Bamber, J.: Can  
732 We Resolve the Basin-Scale Sea Level Trend Budget From GRACE Ocean Mass?, *Journal of*  
733 *Geophysical Research: Oceans*, 125, e2019JC015535, <https://doi.org/10.1029/2019JC015535>,  
734 2020.



735 Storto, A. and Yang, C.: Acceleration of the ocean warming from 1961 to 2022 unveiled by  
736 large-ensemble reanalyses, *Nat Commun*, 15, 545, [https://doi.org/10.1038/s41467-024-44749-](https://doi.org/10.1038/s41467-024-44749-7)  
737 7, 2024.

738 Sun, Y., Riva, R., and Ditmar, P.: Optimizing estimates of annual variations and trends in  
739 geocenter motion and  $J_2$  from a combination of GRACE data and geophysical models, *J.*  
740 *Geophys. Res. Solid Earth*, 121, 8352–8370, <https://doi.org/10.1002/2016JB013073>, 2016.

741 Tapley, B., Watkins, M., Flechtner, F., Reigber, C., Bettadpur, S., Rodell, M., Sasgen, I.,  
742 Famiglietti, J., Landerer, F., Chambers, D., Reager, J., Gardner, A., Save, H., Ivins, E.,  
743 Swenson, S., Boening, C., Dahle, C., Wiese, D., Dobslaw, H., and Velicogna, I.: Contributions  
744 of GRACE to understanding climate change, *Nature Climate Change*, 5,  
745 <https://doi.org/10.1038/s41558-019-0456-2>, 2019.

746 Thierry, V., Claustre, H., Pasqueron De Fommervault, O., Zilberman, N., Johnson, K. S., King,  
747 B. A., Wijffels, S. E., Bhaskar, U. T. V. S., Balmaseda, M. A., Belbeoch, M., Bollard, M.,  
748 Boutin, J., Boyd, P., Cancouët, R., Chai, F., Ciavatta, S., Crane, R., Cravatte, S., Dall’Olmo,  
749 G., Desbruyères, D., Durack, P. J., Fassbender, A. J., Fennel, K., Fujii, Y., Gasparin, F.,  
750 González-Santana, A., Gourcuff, C., Gray, A., Hewitt, H. T., Jayne, S. R., Johnson, G. C.,  
751 Kolodziejczyk, N., Le Boyer, A., Le Traon, P.-Y., Llovel, W., Lozier, M. S., Lyman, J. M.,  
752 McDonagh, E. L., Martin, A. P., Meyssignac, B., Mogensén, K. S., Morris, T., Oke, P. R.,  
753 Smith, W. O., Owens, B., Poffa, N., Post, J., Roemmich, D., Rykaczewski, R. R.,  
754 Sathyendranath, S., Scanderbeg, M., Scheurle, C., Schofield, O., Von Schuckmann, K.,  
755 Scourse, J., Sprintall, J., Suga, T., Tonani, M., Van Wijk, E., Xing, X., and Zuo, H.: Advancing  
756 ocean monitoring and knowledge for societal benefit: the urgency to expand Argo to OneArgo  
757 by 2030, *Front. Mar. Sci.*, 12, 1593904, <https://doi.org/10.3389/fmars.2025.1593904>, 2025.

758 Wang, C., Dong, S., and Munoz, E.: Seawater density variations in the North Atlantic and the  
759 Atlantic meridional overturning circulation, *Clim Dyn*, 34, 953–968,  
760 <https://doi.org/10.1007/s00382-009-0560-5>, 2010.



761 WCRP: Global sea-level budget 1993–present, *Earth System Science Data*, 10, 1551–1590,  
762 <https://doi.org/10.5194/essd-10-1551-2018>, 2018.

763 Wong, A. P. S., Gilson, J., and Cabanes, C.: Argo salinity: bias and uncertainty evaluation,  
764 *Earth System Science Data*, 15, 383–393, <https://doi.org/10.5194/essd-15-383-2023>, 2023.

765 Wunsch, C., Ponte, R. M., and Heimbach, P.: Decadal Trends in Sea Level Patterns: 1993–  
766 2004, *Journal of Climate*, 20, 5889–5911, <https://doi.org/10.1175/2007JCLI1840.1>, 2007.

767 Zuo, H., Balmaseda, M. A., Tietsche, S., Mogensen, K., and Mayer, M.: The ECMWF  
768 operational ensemble reanalysis–analysis system for ocean and sea ice: a description of the  
769 system and assessment, *Ocean Science*, 15, 779–808, <https://doi.org/10.5194/os-15-779-2019>,  
770 2019.

771

772

773